

Inactivating *Icmt* ameliorates K-RAS–induced myeloproliferative disease

*Annika M. Wahlstrom,¹ *Briony A. Cutts,¹ Meng Liu,^{1,2} Annika Lindskog,¹ Christin Karlsson,¹ Anna-Karin M. Sjogren,¹ Karin M. E. Andersson,¹ Stephen G. Young,³ and Martin O. Bergo¹

¹Wallenberg Laboratory, Institute of Medicine, Sahlgrenska University Hospital, Gothenburg, Sweden; ²Department of Neurosurgery, Qilu Hospital, Shandong University, Jinan, China; and ³Departments of Medicine and Human Genetics, David Geffen School of Medicine, University of California, Los Angeles

Hyperactive signaling through the RAS proteins is involved in the pathogenesis of many forms of cancer. The RAS proteins and many other intracellular signaling proteins are either farnesylated or geranylgeranylated at a carboxyl-terminal cysteine. That isoprenylcysteine is then carboxyl methylated by isoprenylcysteine carboxyl methyltransferase (ICMT). We previously showed that inactivation of *Icmt* mislocalizes the RAS proteins away from the plasma membrane and blocks RAS transformation of mouse

fibroblasts, suggesting that ICMT could be a therapeutic target. However, nothing is known about the impact of inhibiting ICMT on the development of malignancies in vivo. In the current study, we tested the hypothesis that inactivation of *Icmt* would inhibit the development or progression of a K-RAS–induced myeloproliferative disease in mice. We found that inactivating *Icmt* reduced splenomegaly, the number of immature myeloid cells in peripheral blood, and tissue infiltration by myeloid cells. Moreover, in the

absence of *Icmt*, the ability of K-RAS–expressing hematopoietic cells to form colonies in methylcellulose without exogenous growth factors was reduced dramatically. Finally, inactivating *Icmt* reduced lung tumor development and myeloproliferation phenotypes in a mouse model of K-RAS–induced cancer. We conclude that inactivation of *Icmt* ameliorates phenotypes of K-RAS–induced malignancies in vivo. (Blood. 2008;112:1357-1365)

Introduction

Activating mutations in *RAS* genes are implicated in the pathogenesis of a large proportion of solid tumors and hematologic malignancies.¹ For example, mutations in *KRAS* and *NRAS* are found in one-third of patients with acute myeloid leukemia (AML), myeloproliferative disorders (MPDs), and myelodysplastic syndromes (MDSs).² Moreover, hyperactive RAS signaling in hematopoietic cells can be elicited by mutations in genes encoding proteins that interact with RAS, such as *FLT3*, *NF1*, and the *BCR/ABL* gene product.³⁻⁵ Thus, the RAS proteins are attractive targets for the treatment of hematologic malignancies.

The RAS proteins and other so-called *CAAX* proteins undergo 3 posttranslational processing steps at a carboxyl-terminal *CAAX* motif. The first step is isoprenylation by farnesyltransferase (FTase) or geranylgeranyltransferase type I (GGTase-I). The second step is endoproteolytic release, by RAS converting enzyme 1 (RCE1), of the 3 amino acids downstream from the isoprenylcysteine. The third step is carboxyl methylation of the newly exposed isoprenylcysteine by isoprenylcysteine carboxyl methyltransferase (ICMT). The processing of the *CAAX* motif increases membrane affinity and promotes protein-protein interactions.⁶

Much effort has focused on trying to block RAS-induced oncogenic transformation by inhibiting FTase. Although some preclinical studies of FTase inhibitors (FTIs) in mouse models showed efficacy and little toxicity,⁷ other studies suggested that these agents might be ineffective in cancer treatment.⁸ Indeed, clinical trials of FTIs in cancer patients have been disappointing. A potential explanation for the poor clinical efficacy of FTase

inhibitors is that both K-RAS and N-RAS are geranylgeranylated by GGTase-I when FTase is inhibited.⁹

We have explored the possibility of inhibiting ICMT as a strategy to prevent the RAS proteins from associating with the plasma membrane and to block RAS-induced transformation of cells. In support of this approach, we found that ICMT is required for the proper membrane targeting of H-, N-, and K-RAS.^{10,11} Moreover, inactivating *Icmt* in mouse fibroblasts inhibited cell growth and K-RAS–induced oncogenic transformation, as judged by both soft agar assays and tumor growth in nude mice.¹¹ Several groups have developed inhibitors of ICMT.¹²⁻¹⁴ One compound, cismethynil, was reported to mislocalize RAS, impair growth factor signaling, and block the anchorage-independent growth of a human cancer cell line.¹⁴

Although these in vitro studies have suggested that ICMT might be an attractive therapeutic target, no studies have yet defined the impact of inhibiting ICMT on the development of RAS-induced malignancies in vivo. In addition, the in vitro studies on ICMT inactivation were performed with cells in which human oncogenic K-RAS was highly overexpressed with an expression vector driven by a strong viral promoter.¹¹ Nothing is yet known about the effect of *Icmt* deficiency on transformation induced by an activating mutation in the *endogenous* K-RAS gene, where the absolute levels of K-RAS expression are lower. To address this issue, we designed studies to test the impact of *Icmt* deficiency on the development and progression of malignancies induced by an activating mutation in the endogenous K-RAS gene.

Submitted June 6, 2007; accepted April 6, 2008. Prepublished online as *Blood* First Edition paper, May 23, 2008; DOI 10.1182/blood-2007-06-094060.

*A.M.W. and B.A.C. contributed equally to this study.

The online version of this article contains a data supplement.

The publication costs of this article were defrayed in part by page charge payment. Therefore, and solely to indicate this fact, this article is hereby marked "advertisement" in accordance with 18 USC section 1734.

© 2008 by The American Society of Hematology

Methods

Mouse breeding

Mice with a conditional *Icmt* knockout allele (*Icmt*^{fl})¹¹ were bred with mice harboring a latent but *Cre*-inducible *Kras2*^{LSL} allele (hereafter designated *K*^{LSL})¹⁵ to generate *Icmt*^{fl/fl}*K*^{LSL} mice. The *K*^{LSL} allele contains an activating mutation in codon 12 and a stop cassette flanked by *loxP* sites (LSL; *loxP*STOP*loxP*) in the promoter. Expression of *Cre* recombinase results in excision of the stop cassette and expression of the mutated *Kras2*^{G12D} allele. *Icmt*^{fl/fl}*K*^{LSL} mice were bred with *Icmt*^{fl/+} mice harboring an interferon-inducible Mx1-*Cre* transgene (designated M) to generate *Icmt*^{fl/+}*K*^{LSL}M and *Icmt*^{fl/fl}*K*^{LSL}M mice. In these mice, *Cre* expression simultaneously activated K-RAS^{G12D} expression and inactivated *Icmt* in bone marrow cells. Inactivation of one *Icmt* allele produces no apparent phenotypes. Littermate mice that did not inherit both the *K*^{LSL} and M alleles were used as controls. The *Icmt*^{fl/fl}*K*^{LSL} mice were also bred with mice harboring the lysozyme M-*Cre* allele (designated LC)¹⁶ to produce *Icmt*^{fl/+}*K*^{LSL}LC and *Icmt*^{fl/fl}*K*^{LSL}LC mice. In the LC mice, *Cre* is expressed in type 2 pneumocytes and myeloid cells.¹⁷ The gene nomenclature used for the different groups of mice refers to the genotype detected in tail DNA at weaning; the genotype after *Cre*-mediated recombination is used to describe homogeneous cell populations (eg, cultured fibroblasts). Mice were maintained on a 129/Sv and C57BL/6 mixed genetic background. Animal procedures were approved by the animal research ethics committee in Gothenburg, Sweden.

Genotyping

Genotyping was performed by PCR amplification of genomic DNA from mouse tail biopsies, tumors, tissues, cultured cells, and colonies from hematopoietic growth assays. The *Icmt*^{fl} allele was detected with forward primer 5'-GGGCGGGACGGACAG-3' and reverse primer 5'-ATGCGCATCTGCCTAAGCTG-3', yielding a 600-bp fragment from the *Icmt*^{fl} allele and a 538-bp fragment from the *Icmt*⁺ allele. The *Icmt*^Δ allele was detected with forward primer 5'-CCGCTCGCTCCGAATCCAG-3' and reverse primer 5'-CTCGTAAACCGACCACCAAT-3'; the amplified fragment was 600 bp. The stop cassette in the *K*^{LSL} allele was detected with forward primer 5'-CCTTTACAAGCGACGACACTGTAGA-3' and reverse primer 5'-AGTAGCCACCATGGCTTGAGTAAGTCTGCA-3'; the amplified fragment was 600 bp. The activated *K*^{G12D} allele was detected with forward primer 5'-GGTAGGTGTTGGGATAGCTG-3' and reverse primer 5'-TCCGAATTCAGTGACTACAGATGTACAGAG-3', yielding a 320-bp fragment from the *K*^{G12D} allele and a 280-bp fragment from the wild-type (*K*⁺) allele. The Mx1-*Cre* transgene was detected with forward primer 5'-GAGCTCCATTCATGTGTGGT-3' and reverse primer 5'-CTAGAGCCTGTTTTGCACGTTTC-3'; the amplified fragment was 1009 bp. The LC allele was detected with forward primer 5'-CTTGGGCTGCCA-GAATTTCTC-3' and reverse primers 5'-TTACAGTCGGCCAGGCTGAC-3' and 5'-CCCAGAAATGCCAGATTACG-3', yielding a 700-bp fragment from the LC allele and a 350-bp fragment from the wild-type (*Lysm*⁺) allele.

Cell proliferation experiments

Mouse embryonic fibroblasts were isolated from *Icmt*^{fl/+}*K*^{LSL} and *Icmt*^{fl/fl}*K*^{LSL} embryos at embryonic (E) day 13.5 to 18.5. Primary (passage 1-3) and spontaneously immortalized (passage 17-27) fibroblasts (5×10^5 cells) were seeded in 60-mm plates and infected with adenoviruses encoding *Cre*- or β -galactosidase (AdRSV*Cre* and AdRSV*nlacZ*, respectively; 10^9 pfu/mL culture medium, Iowa University, Iowa City, IA). For the immortalized cells, 2×10^4 cells of each genotype were seeded in 12-well plates in triplicate; at various times, the cells were trypsinized and counted (NucleoCounter, Chemometec, Allerod, Denmark). For focus formation assays, 20 000 cells were plated in 6-well plates in triplicate, and foci were counted on day 12. For the primary cells, 10^4 cells of each genotype were seeded in 100-mm plates and counted on day 23. Cells on plastic culture dishes were photographed with a Leica DMIL light microscope using a

Leica DC200 digital camera (Leica, Wetzlar, Germany) in conventional culture medium.

Western blots

GTP-bound RAS proteins were isolated with the RAS Activation kit (Assay Designs, Ann Arbor, MI). Membrane and soluble fractions from splenocytes were separated by ultracentrifugation as described.¹¹ CD11b-positive splenocytes were isolated with the OctoMACS system (Miltenyi Biotec, Bergisch Gladbach, Germany). Unfractionated and CD11b-positive splenocytes were serum-starved for 4 hours and then stimulated with granulocyte-macrophage colony-stimulating factor (GM-CSF) for 10 minutes. Total protein extracts from fibroblasts, unfractionated and CD11b-positive splenocytes, and cellular fractions from splenocytes were size-fractionated on 10% to 20% sodium dodecyl sulfate polyacrylamide gels (Criterion, Bio-Rad, Hercules, CA). The proteins were transferred to a nitrocellulose membrane and incubated with antibodies recognizing K-RAS (234-4.2, Merck, Darmstadt, Germany), total RAS (Assay Designs), ACTIN (A2066, Sigma-Aldrich, St Louis, MO), phosphorylated ERK1/2 (9101), total ERK1/2 (9102), phosphorylated MEK1/2^{Ser217/221} (9121), total MEK1/2 (9122), phosphorylated AKT^{Ser473} (9271), or total AKT (9272, Cell Signaling, Danvers, MA). Protein bands were visualized with horseradish peroxidase-conjugated secondary antibodies (NA931 and NA934, GE Healthcare, Little Chalfont, United Kingdom).

In vivo experiments

The K-RAS-induced MPD model has been described previously.¹⁸⁻²⁰ Groups of 3-week-old *Icmt*^{fl/+}*K*^{LSL}M, *Icmt*^{fl/fl}*K*^{LSL}M, and control mice were injected with 400 μ g of polyinosinic-polycytidylic acid (pI-pC; Sigma-Aldrich) once every 2 days for a total of 4 injections to induce *Cre* expression in bone marrow cells. Blood was drawn from a tail vein before the first pI-pC injection (time point 0) and once per week for up to 14 weeks. The blood was analyzed with a Hemavet 950FS cell counter (Drew Scientific, Dallas, TX) and by manual differential counts of May-Grünwald-Giemsa-stained smears. At various times, groups of mice were killed and tissues harvested. For the K-RAS-induced lung cancer and myeloproliferation model, groups of *Icmt*^{fl/+}*K*^{LSL}LC, *Icmt*^{fl/fl}*K*^{LSL}LC, and control mice were killed at 20 to 24 days of age. Other groups of mice were monitored until showing signs of severe shortness of breath resulting from lung tumors and then killed for harvesting of tissues.

Fluorescence-activated cell sorting

Splenocytes from *Icmt*^{fl/+}*K*^{LSL}M, *Icmt*^{fl/fl}*K*^{LSL}M, and control mice were isolated 7 weeks after pI-pC injections and incubated with antibodies recognizing cell-surface antigens CD11b (550993), CD45 (557659), and Gr-1 (553129) (BD Biosciences, San Jose, CA), and analyzed in a FACSaria (BD Biosciences). Data were analyzed with FACS Diva software (BD Biosciences).

Hematopoietic colony assays

Splenocytes (10^5) and bone marrow cells (2×10^4) were cultured in duplicate wells in methylcellulose medium in the absence (MethoCult M3231, StemCell Technologies, Vancouver, BC) and presence of growth factors (stem cell factor (SCF), interleukin-3 (IL-3), interleukin-6 (IL-6), and erythropoietin (EPO) (MethoCult M3434)), or in the presence of GM-CSF: colonies were typed and counted on day 10. Hematopoietic cells were also cultured in methylcellulose medium (MethoCult M3234) supplemented with EPO and burst-forming unit erythroid (BFU-E) colonies were counted on day 7. Genomic DNA from single colonies was extracted and used for genotyping, and cytospin preparations of cells in individual colonies were stained with May-Grünwald-Giemsa and analyzed by light microscopy (Zeiss Axioplan 2, Oberkochen, Germany).

Histology

Tissues were fixed in 4% formalin, dehydrated in 70% to 100% ethanol, cleared in xylene, and embedded in paraffin. Sections (4-5 μ m) were

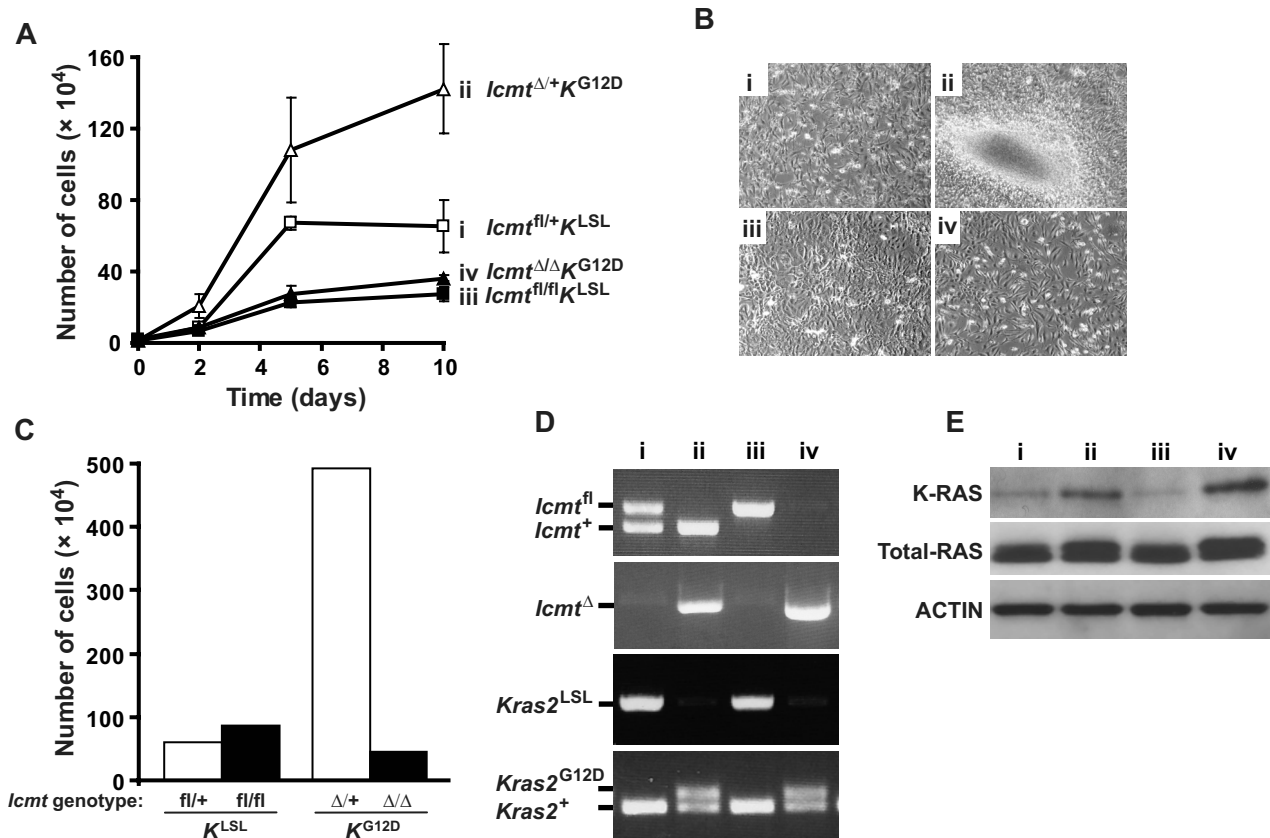


Figure 1. Inactivation of *Icmf* inhibits cell proliferation induced by expression of an endogenous K-RAS^{G12D} allele in mouse embryonic fibroblasts. (A) Proliferation of immortalized *Icmf*^{fl/+}*K*^{L^{SL}} and *Icmf*^{fl/fl}*K*^{L^{SL}} cells infected with Cre- and β-gal-adenoviruses. Cre-adenovirus-treatment of *Icmf*^{fl/+}*K*^{L^{SL}} and *Icmf*^{fl/fl}*K*^{L^{SL}} fibroblasts produced *Icmf*^{Δ/+}*K*^{G12D} and *Icmf*^{Δ/Δ}*K*^{G12D} cells that expressed endogenous K-RAS^{G12D} and that had one or both *Icmf* alleles inactivated, respectively. Data are mean plus or minus SEM of one cell line assayed in triplicate. Similar results were obtained in 5 independent experiments. (B) Cells from a focus formation assay taken 12 days after plating (original magnification ×10; 0.22 NA objective). (C) Proliferation of primary *Icmf*^{fl/+}*K*^{L^{SL}} and *Icmf*^{fl/fl}*K*^{L^{SL}} cells infected with β-gal- (2 left bars) and Cre-adenoviruses (2 right bars). A total of 10⁴ cells were plated and counted after 23 days. Data are one cell line for *Icmf*^{fl/+}*K*^{L^{SL}} and the mean of 2 cell lines for *Icmf*^{fl/fl}*K*^{L^{SL}}. (D) PCR amplification of genomic DNA from cells of a typical experiment in panel A showing the deletion of the *Icmf*^{fl} allele and the stop cassette in the promoter of the *Kras2*^{L^{SL}} allele and the appearance of the *Icmf*^Δ band and the activated *Kras2*^{G12D} band in Cre-adenovirus-treated cells (lanes 2 and 4). (E) Western blots showing levels of K-RAS, total RAS, and ACTIN in total cellular extracts from cells in panel A. Similar results were obtained with a different pair of cell lines. For panels B, D, and E, the genotypes of cell lines i through iv are shown in panel A.

stained with hematoxylin and eosin and analyzed by light microscopy. Slides were photographed with an AxioCam HRC digital camera mounted on an Axiophot microscope (Zeiss) in Mountex mounting medium (Histolab Products, Gothenburg, Sweden).

Statistical analyses

Data were plotted as mean and SEM. Differences in the concentrations of immature white blood cells, tissue weights, percentages of CD11b/Gr-1 double-positive splenocytes, colony-forming ability of hematopoietic cells, and cell size were determined with one-way analysis of variance and Tukey post-hoc test for multiple comparisons; survival was assessed by the log-rank test.

Results

Inactivating *Icmf* blocks proliferation induced by endogenous oncogenic K-RAS in mouse fibroblasts

We previously showed that inactivating *Icmf* inhibits the proliferation of immortalized fibroblasts overexpressing an oncogenic form of human K-RAS. To determine whether inactivation of *Icmf* would inhibit the proliferation of fibroblasts expressing oncogenic K-RAS from the endogenous promoter, we isolated *Icmf*^{fl/+}*K*^{L^{SL}} and *Icmf*^{fl/fl}*K*^{L^{SL}} embryonic fibroblasts.

Cre-adenovirus treatment of immortalized *Icmf*^{fl/+}*K*^{L^{SL}} fibroblasts yielded *Icmf*^{Δ/+}*K*^{G12D} cells (with expression of K-RAS^{G12D} from the endogenous promoter and with one *Icmf* allele inactivated) and resulted in rapid cell proliferation and partial transformation (Figure 1A,B), consistent with previous studies using *K*^{L^{SL}} fibroblasts.^{20,21} In contrast, Cre-adenovirus treatment of *Icmf*^{fl/fl}*K*^{L^{SL}} fibroblasts (yielding *Icmf*^{Δ/Δ}*K*^{G12D} cells, with both *Icmf* alleles inactivated) blocked the K-RAS^{G12D}-induced increase in proliferation and partial transformation (Figure 1A,B). The *Icmf*^{Δ/+}*K*^{G12D} cells formed 17 plus or minus 2 foci in a focus formation assay: the *Icmf*^{Δ/Δ}*K*^{G12D} cells, and the parental *Icmf*^{fl/+}*K*^{L^{SL}} and *Icmf*^{fl/fl}*K*^{L^{SL}} cells, did not form foci. In primary *Icmf*^{fl/+}*K*^{L^{SL}} fibroblasts, Cre-adenovirus treatment resulted in rapid cell growth and immortalization: these phenotypes were abolished by inactivating *Icmf* in primary *Icmf*^{fl/fl}*K*^{L^{SL}} fibroblasts (Figure 1C; data not shown). Figure 1D demonstrates the complete inactivation of the *Icmf*^{fl} allele and the activation of the *Kras2*^{G12D} allele in Cre-adenovirus-treated fibroblasts. Figure 1E shows increased levels of K-RAS protein in the *Icmf*^{Δ/+}*K*^{G12D} and *Icmf*^{Δ/Δ}*K*^{G12D} fibroblasts (lanes 2 and 4) compared with the parental *Icmf*^{fl/+}*K*^{L^{SL}} and *Icmf*^{fl/fl}*K*^{L^{SL}} fibroblasts, as judged by Western blotting with K-RAS and pan-RAS antibodies (Figure 1E).

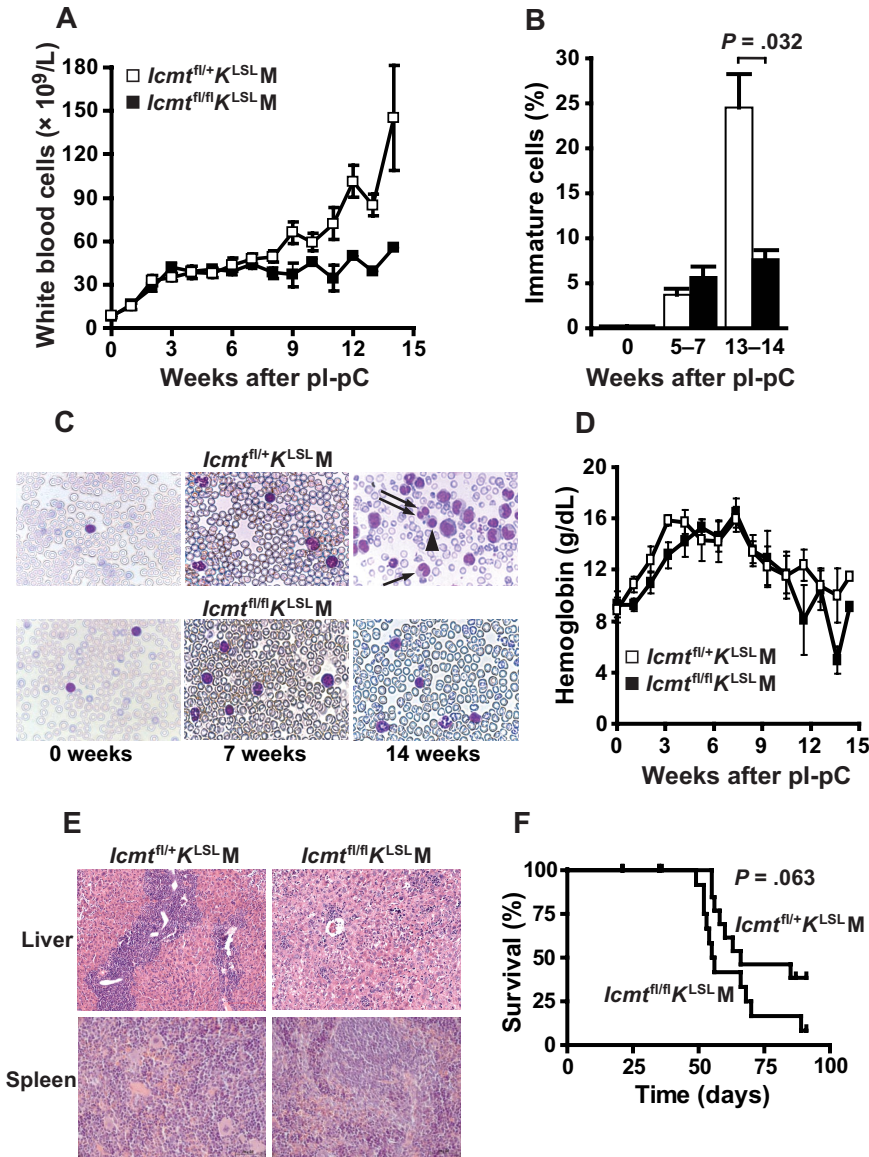


Figure 2. *Icm1* deficiency reduces the accumulation of immature myeloid cells and tissue infiltration in mice with K-RAS–induced MPD. (A) White blood cell counts of *Icm1*^{fl/+}*K*^{LSL}*M* and *Icm1*^{fl/fl}*K*^{LSL}*M* mice. Blood was analyzed before and weekly after pi-pC injections. (*Icm1*^{fl/+}*K*^{LSL}*M*: week 0–8, n = 11–19; week 9–14, n = 4–6; *Icm1*^{fl/fl}*K*^{LSL}*M*: week 0–7, n = 7–20; week 8–14, n = 1–5). (B) White blood cells were evaluated in blood smears from *Icm1*^{fl/+}*K*^{LSL}*M* (□) and *Icm1*^{fl/fl}*K*^{LSL}*M* mice (■) before pi-pC injections (n = 6–7), at 5 to 7 weeks (n = 5), and at 13 to 14 weeks after pi-pC injections (n = 2–3). Shown is the percentage of immature cells (ie, myeloblasts, myelocytes, metamyelocytes, band cells, and pelgeroid cells). (C) Photographs of typical blood smears from panel B (original magnification ×100; 1.30 NA oil objective). (Top right panel) → represents band cell; ⇌, pelgeroid cell; ▲, erythroblast. The large cell to the right of the erythroblast is a myeloblast. (D) Hemoglobin concentrations measured in the blood samples shown in panel A. (E) Hematoxylin and eosin–stained sections of liver and spleen of mice killed 13 weeks after pi-pC injections (original magnification ×20; 0.50 NA objective). (F) Kaplan–Meier curve showing survival of *Icm1*^{fl/+}*K*^{LSL}*M* (n = 21) and *Icm1*^{fl/fl}*K*^{LSL}*M* (n = 22) mice.

Inactivating *Icm1* reduces tissue infiltration and accumulation of immature myeloid cells in peripheral blood in mice with K-RAS–induced MPD

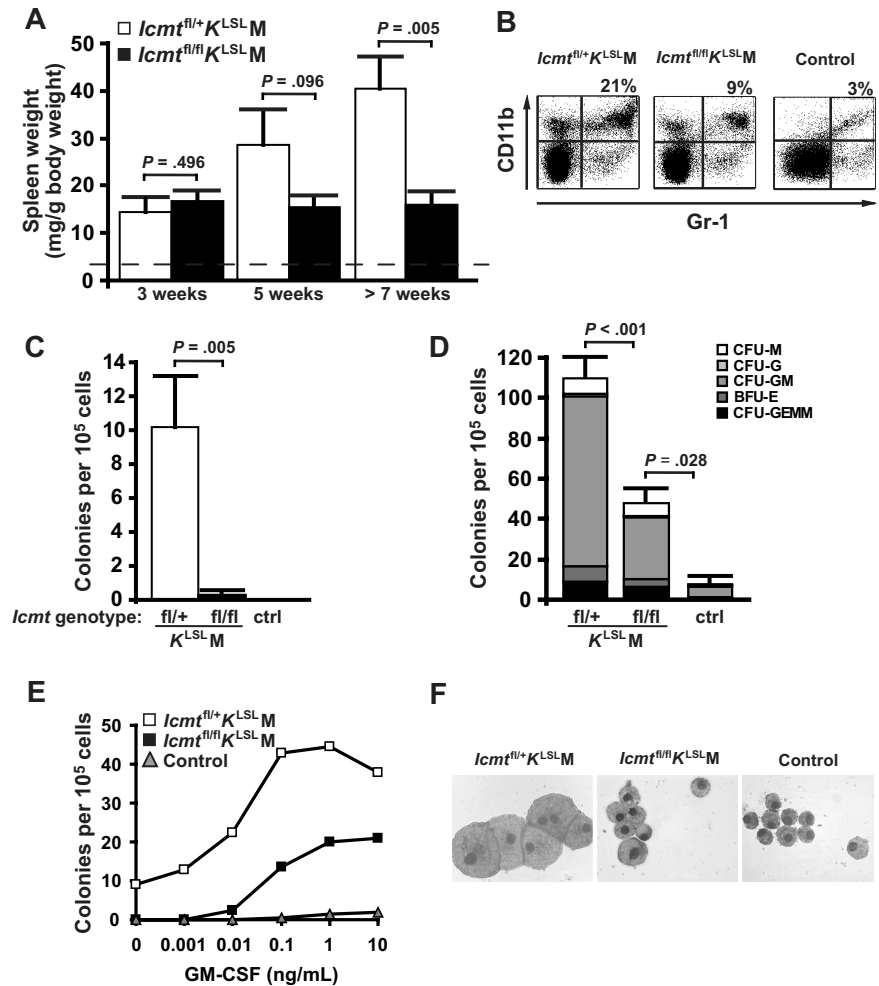
To define the impact of *Icm1* deficiency on the development and progression of K-RAS–induced MPD, we injected *Icm1*^{fl/+}*K*^{LSL}*M* and *Icm1*^{fl/fl}*K*^{LSL}*M* mice with pi-pC and monitored them for up to 14 weeks. The pi-pC injections “switched on” the expression of K-RAS^{G12D} and inactivated one *Icm1* allele in the case of the *Icm1*^{fl/+}*K*^{LSL}*M* mice and 2 alleles in the case of the *Icm1*^{fl/fl}*K*^{LSL}*M* mice. In previous studies, we showed that inactivation of the conditional *Icm1* allele eliminates ICMT enzymatic activity, mislocalizes the RAS proteins away from the plasma membrane, and results in a striking accumulation of “methylatable” substrates within cells (ie, cellular proteins that can be methylated by recombinant ICMT).¹¹ In addition, the Mx1-Cre–induced inactivation of *Icm1* produced no apparent phenotypes in mice, even over many months of observation (A.M.W. and M.O.B., unpublished data, 2007).¹⁰

From 0 to 7 weeks after pi-pC injections, both *Icm1*^{fl/+}*K*^{LSL}*M* and *Icm1*^{fl/fl}*K*^{LSL}*M* mice developed signs of MPD with increased white blood cell counts (Figure 2A) but with only a small

proportion (4%–6%) of immature myeloid cells in peripheral blood (Figure 2B,C). After 7 weeks, the white blood cell counts increased more rapidly in the *Icm1*^{fl/+}*K*^{LSL}*M* compared with the *Icm1*^{fl/fl}*K*^{LSL}*M* mice. Moreover, 13 to 14 weeks after pi-pC treatment, the percentage of immature myeloid cells in blood from the *Icm1*^{fl/+}*K*^{LSL}*M* mice increased to 25%, whereas it remained less than 8% in the *Icm1*^{fl/fl}*K*^{LSL}*M* mice (Figure 2B,C; *P* = .032). Hemoglobin levels in both *Icm1*^{fl/+}*K*^{LSL}*M* and *Icm1*^{fl/fl}*K*^{LSL}*M* mice increased during the first 7 weeks after pi-pC injections. After 7 weeks, hemoglobin levels decreased steadily and visibly ill mice were usually anemic (Figure 2D). The *Icm1*^{fl/+}*K*^{LSL}*M* mice exhibited infiltration of myeloid cells in the liver and disruption of the splenic cytoarchitecture; in *Icm1*^{fl/fl}*K*^{LSL}*M* mice, these phenotypes were markedly reduced (Figure 2E). Despite inhibiting the progression and severity of MPD phenotypes, the inactivation of *Icm1* did not improve survival. The median survival was 66 days for *Icm1*^{fl/+}*K*^{LSL}*M* mice (n = 21) and 55 days for the *Icm1*^{fl/fl}*K*^{LSL}*M* mice (n = 22) (*P* > .05; Figure 2F).

As expected from previous studies with the K-RAS–induced MPD,¹⁹ both *Icm1*^{fl/+}*K*^{LSL}*M* and *Icm1*^{fl/fl}*K*^{LSL}*M* mice developed lesions in other tissues, such as malignant thymic lymphoma,

Figure 3. Inactivation of *Icmt* reduces splenomegaly and colony growth of splenocytes in mice with K-RAS–induced MPD. (A) Spleen weight of *Icmt*^{fl/+}*K*^{LSL}M (n = 3, 5, and 9 at the 3 indicated times, respectively) and *Icmt*^{fl/fl}*K*^{LSL}M mice (n = 4, 6, and 9). Average spleen weight of wild-type mice (dashed line; n = 20) was 3 mg/g body weight. (B) Flow cytometry showing an increased percentage of CD11b/Gr-1 double-positive cells in spleens of *Icmt*^{fl/+}*K*^{LSL}M compared with *Icmt*^{fl/fl}*K*^{LSL}M and wild-type mice. Shown are representative scatter plots from one mouse of each genotype and the mean percentage of double-positive cells (n = 4 for all genotypes). The increase in double-positive cells in the spleens of *Icmt*^{fl/+}*K*^{LSL}M mice was statistically significant (*P* = .043 vs *Icmt*^{fl/fl}*K*^{LSL}M; *P* = .009 vs control). (C,D) Methylcellulose colony assays of splenocytes (n = 3–4) cultured in the absence (C) and presence (D) of exogenous growth factors (SCF, IL-3, IL-6, and EPO). CFU indicates colony-forming unit; GEMM, granulocyte-erythroid-macrophage-megakaryocyte; BFU-E, burst-forming unit erythroid; GM, granulocyte-macrophage; G, granulocyte; M, macrophage. (E) Colony growth of splenocytes (n = 3–4 for each genotype) seeded in methylcellulose at the indicated concentrations of GM-CSF. (F) May-Grünwald-Giemsa–stained cytopins of individual colonies from experiment in panel D (original magnification ×100; 1.30 NA oil objective).



adenocarcinoma of the lung, and large papillomas in the gastrointestinal tract (Figure S1, available on the *Blood* website; see the Supplemental Materials link at the top of the online article). The lesions in other tissues were not surprising because the Mx1-*Cre* transgene induces recombination in many cell types other than hematopoietic cells, although at a lower level.²² We speculated that the reason the *Icmt*^{fl/fl}*K*^{LSL}M mice exhibited reduced MPD phenotypes (ie, phenotypes in spleen and bone marrow), but no improvement in survival could be related to the lesions in other tissues (where there could be a high likelihood of K-RAS activation without the complete inactivation of *Icmt*). To address this issue, we genotyped tissues and lesions from pI-pC–injected *Icmt*^{fl/fl}*K*^{LSL}M mice by PCR of genomic DNA. As expected, in spleen and bone marrow, the *K*^{G12D} allele was activated and *Icmt* was almost completely inactivated (Figure S1). However, isolated lesions from all other tissues showed incomplete inactivation of *Icmt* (Figure S1).

***Icmt* deficiency reduces splenomegaly and growth factor–independent colony growth of splenocytes from mice with K-RAS–induced MPD**

Three weeks after pI-pC injections, the *Icmt*^{fl/+}*K*^{LSL}M and *Icmt*^{fl/fl}*K*^{LSL}M mice had similar spleen weights (Figure 3A). Over the following 2 weeks (week 4–5), spleen weight in *Icmt*^{fl/+}*K*^{LSL}M mice doubled but remained unchanged in *Icmt*^{fl/fl}*K*^{LSL}M mice. In mice killed 7 to 13 weeks after pI-pC injections, spleen weight was

2.6-fold higher in *Icmt*^{fl/+}*K*^{LSL}M mice compared with *Icmt*^{fl/fl}*K*^{LSL}M mice (Figure 3A; *P* = .005). Fluorescence-activated cell sorting analysis of splenocytes from *Icmt*^{fl/+}*K*^{LSL}M mice showed an increased proportion of CD11b and Gr-1 double-positive cells compared with both *Icmt*^{fl/fl}*K*^{LSL}M (*P* = .043) and control (*P* = .009) mice (Figure 3B). As expected from previous studies with the K-RAS–induced MPD,^{18–20} splenocytes from pI-pC–injected *Icmt*^{fl/+}*K*^{LSL}M mice were able to form colonies in methylcellulose without exogenous growth factors (Figure 3C). In contrast, the ability of splenocytes from *Icmt*^{fl/fl}*K*^{LSL}M mice to form colonies without growth factors was reduced by more than 95% (Figure 3C; *P* = .005). In the presence of growth factors (SCF, IL-3, IL-6, and EPO), colony formation by *Icmt*^{fl/fl}*K*^{LSL}M splenocytes was reduced by 56% compared with *Icmt*^{fl/+}*K*^{LSL}M splenocytes (*P* = .005) but was still higher than with control splenocytes (*P* = .028; Figure 3D); the splenocyte colonies were primarily granulocyte-macrophage colony-forming units (CFU-GM). The *Icmt*^{fl/fl}*K*^{LSL}M splenocytes formed colonies at high concentrations of GM-CSF, but not at low concentrations, which induced numerous colonies from *Icmt*^{fl/+}*K*^{LSL}M splenocytes (Figure 3E); control splenocytes did not form colonies in response to GM-CSF (Figure 3E). The *Icmt*^{fl/+}*K*^{LSL}M CFU-GM colonies were composed of large macrophage-like cells; the cells in *Icmt*^{fl/fl}*K*^{LSL}M colonies were approximately 50% smaller (Figure 3F; *P* < .001) and resembled cells in colonies from control splenocytes.

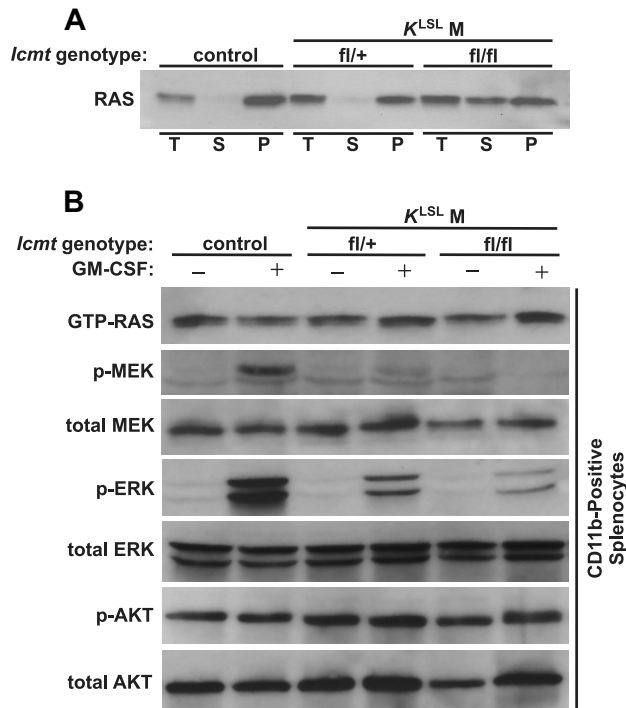


Figure 4. Mislocalization of RAS proteins in *Icm*-deficient splenocytes and analyses of downstream RAS effectors in CD11b-positive splenocytes. (A) Intracellular localization of RAS proteins in splenocytes. Total cell extracts (T) from splenocytes were fractionated into soluble (S) and membrane (P) fractions and analyzed on Western blots with a pan-RAS antibody. Note the accumulation of RAS proteins in the soluble (S) fraction in splenocytes of *Icm*^{fl/fl}*K*^{LSL}*M* mice. (B) Western blots showing levels of GTP-bound RAS and downstream effectors in serum-starved and GM-CSF-stimulated CD11b-positive splenocytes pooled from mice of the same genotype (control, n = 5; *Icm*^{fl/+}*K*^{LSL}*M*, n = 3; *Icm*^{fl/fl}*K*^{LSL}*M*, n = 3).

To determine the intracellular localization of the RAS proteins in *Icm*-deficient cells in vivo, we harvested splenocytes from mice 5 weeks after injections of pI-pC and then isolated membrane and soluble fractions. In splenocytes from control and *Icm*^{fl/+}*K*^{LSL}*M* mice, essentially all RAS proteins were in the membrane fraction (Figure 4A). In contrast, in *Icm*^{fl/fl}*K*^{LSL}*M* splenocytes, a substantial proportion of the RAS proteins were in the soluble fraction (Figure 4A). We assessed the activation of RAS and downstream effectors in unfractionated splenocytes and observed higher levels of basal and GM-CSF-stimulated phosphorylated ERK in *Icm*^{fl/+}*K*^{LSL}*M* splenocytes than in control and *Icm*^{fl/fl}*K*^{LSL}*M* splenocytes (Figure S2). However, because the proportion of CD11b-positive splenocytes varied from 3% to 21% between the 3 groups of mice, we isolated and analyzed CD11b cells (Figure 4B). RAS-GTP was present in both serum-starved and GM-CSF-stimulated CD11b cells and varied little between the 3 groups of mice. Despite the presence of RAS-GTP, the levels of phosphorylated MEK and ERK in serum-starved CD11b cells were low. In control CD11b cells, the phosphorylation of MEK and ERK after GM-CSF stimulation was robust. However, the phosphorylation of both MEK and ERK was reduced in *Icm*^{fl/+}*K*^{LSL}*M* cells and was further reduced in *Icm*^{fl/fl}*K*^{LSL}*M* cells. Levels of phosphorylated AKT were high in serum-starved CD11b cells from the 3 groups of mice and did not change after GM-CSF stimulation. In keeping with the results of an earlier study,¹⁸ there were no differences in the activation of ERK and AKT in bone marrow cells between the 3 groups of mice (not shown).

Inactivation of *Icm* inhibits growth factor-independent colony growth of myeloid and erythroid progenitors in bone marrow

Consistent with the results from splenocytes, the ability of bone marrow cells from pI-pC-injected *Icm*^{fl/fl}*K*^{LSL}*M* mice to form colonies in the absence of growth factors was reduced by approximately 95% compared with cells from *Icm*^{fl/+}*K*^{LSL}*M* mice (Figure 5A; *P* = .001). Surprisingly, however, in the presence of growth factors (SCF, IL-3, IL-6, and EPO), colony growth of bone marrow cells from *Icm*^{fl/fl}*K*^{LSL}*M* mice was actually increased compared with *Icm*^{fl/+}*K*^{LSL}*M* (*P* = .006) and control (*P* = .007) mice (Figure 5B; the colonies were CFU-GM). To determine whether inactivation of *Icm* would also increase colony growth of normal bone marrow cells (ie, cells that did not express K-RAS^{G12D}), we harvested bone marrow cells 2 weeks after pI-pC injections of *Icm*^{fl/fl}*M* and control *Icm*^{fl/+}*M* mice. Bone marrow cells from *Icm*^{fl/fl}*M* mice formed 33% more colonies than cells from *Icm*^{fl/+}*M* mice (Figure 5C; *P* = .023) in the presence of growth factors. We assessed the sensitivity of bone marrow cells to GM-CSF. At low concentrations of GM-CSF (0-0.1 ng/mL), bone marrow cells from *Icm*^{fl/fl}*K*^{LSL}*M* mice formed fewer colonies than cells from *Icm*^{fl/+}*K*^{LSL}*M* mice. At saturating concentrations of GM-CSF (> 1 ng/mL), *Icm*-deficient bone marrow cells, both with (Figure 5D) and without (Figure 5E) K-RAS^{G12D}, formed more colonies than cells from heterozygous *Icm*-deficient and control mice.

Previous studies have shown that bone marrow cells expressing K-RAS^{G12D} are hypersensitive to EPO and exhibit EPO-independent production of BFU-E colonies.²³ Consistent with those studies, bone marrow cells from *Icm*^{fl/+}*K*^{LSL}*M* mice showed robust BFU-E formation both in the absence and presence of EPO (Figure 5F). In contrast, the EPO sensitivity of bone marrow cells from *Icm*^{fl/fl}*K*^{LSL}*M* mice was similar to control (Figure 5F). We found similar results with splenocytes (not shown).

Genotyping of genomic DNA from individual colonies demonstrated that both of the floxed *Icm* alleles were inactivated when hematopoietic cells of *Icm*^{fl/fl}*K*^{LSL}*M* and *Icm*^{fl/fl}*M* mice were used (Figure 5G,H).

Knockout of *Icm* eliminates myeloproliferation and reduces lung tumor development in a second line of K-RAS^{G12D} mice

To further define the impact of *Icm* deficiency on the development of K-RAS-induced malignancies in vivo, we bred *Icm*^{fl/fl}*K*^{LSL}*M* mice with mice expressing *Cre* recombinase in type 2 pneumocytes and myeloid cells (LC, lysozyme M-*Cre*).¹⁶ *K*^{LSL}*LC* mice develop a rapidly progressing lung cancer. The *K*^{LSL}*LC* mice die or have to be killed at 3 weeks of age, resulting from respiratory failure from the obliteration of the alveolar architecture.¹⁷ Consistent with those findings, the median survival of *Icm*^{fl/+}*K*^{LSL}*LC* mice was 22 days (Figure 6A), and lung weight was increased 8-fold compared with control mice. The tumor histology ranged from diffuse hyperplasia to adenoma and adenocarcinoma with very few areas of normal alveolar structures (Figure S3A-C). Survival was improved in the *Icm*^{fl/fl}*K*^{LSL}*LC* mice (median survival, 50 days, *P* < .001; Figure 6A) and lung weight was decreased by 33% compared with the *Icm*^{fl/+}*K*^{LSL}*LC* mice (*P* < .001). Lung histology of 3-week-old *Icm*^{fl/fl}*K*^{LSL}*LC* mice ranged from nests of atypical adenomatous hyperplasia to diffuse hyperplasia, but the lungs retained areas of normal histology (Figure S3D,E). Normal lung histology is shown in Figure S3F.

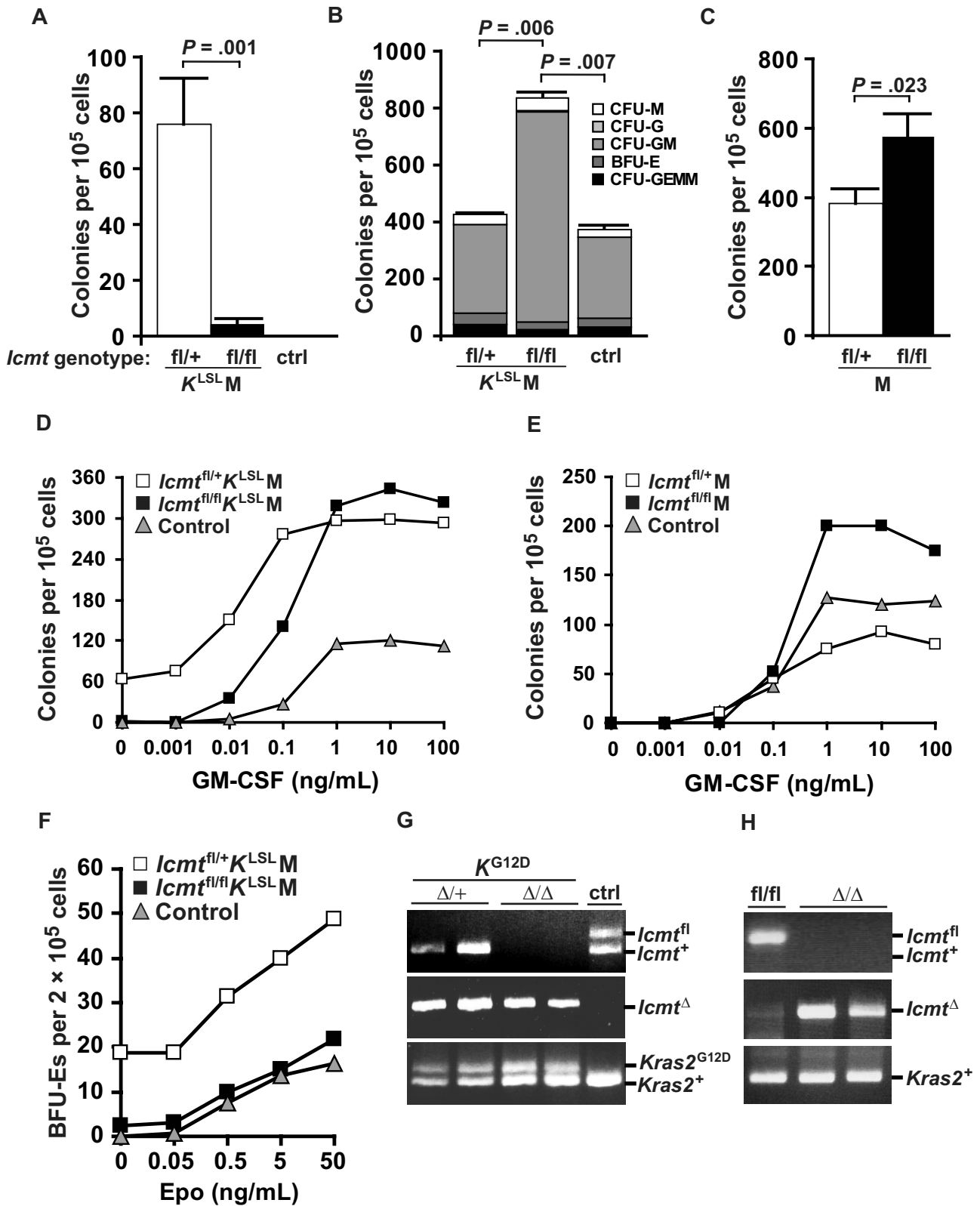


Figure 5. Knockout of *Icm1* reduces growth factor-independent colony growth of bone marrow cells from mice with K-RAS-induced MPD. (A,B,D) Methylcellulose colony assays of bone marrow cells (n = 3-5 for each genotype) cultured in the absence (A) and presence (B) of growth factors (SCF, IL-3, IL-6, and EPO), and the indicated concentrations of GM-CSF (D). (C,E) Colony growth of bone marrow cells from *Icm1^{fl/+}M* (n = 3) and *Icm1^{fl/fl}M* mice (n = 3) (without the *Kras2^{LSL}* allele) cultured in the presence of growth factors (C) or the indicated concentrations of GM-CSF (E). (F) BFU-E formed by bone marrow cells (n = 2 for each genotype) cultured in the indicated concentrations of EPO. (G,H) PCR amplification of genomic DNA from individual colonies. The genomic DNA used in panel G is from colonies from experiments in Figures 3D and 5B. DNA used in panel H is from experiments in panel C.

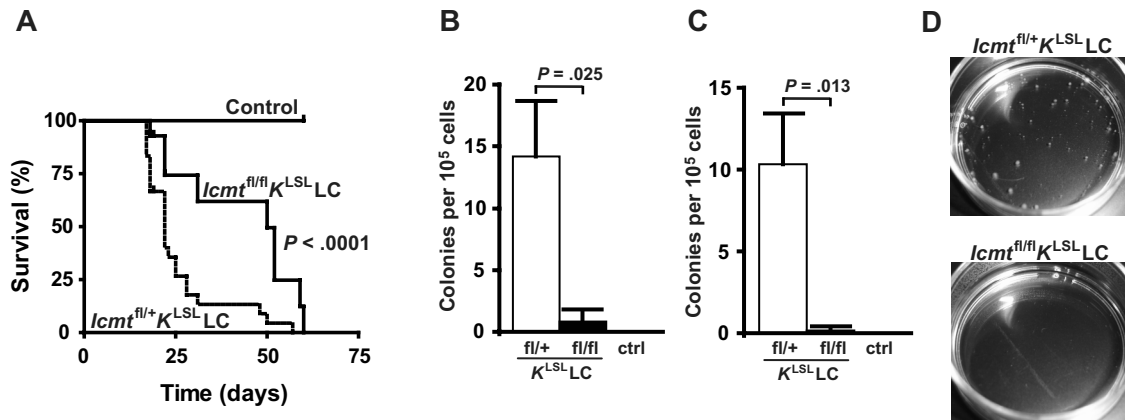


Figure 6. Inactivation of *Icmf* improves survival and reduces autonomous colony growth of hematopoietic cells in a second model of K-RAS-induced malignancies. (A) Survival of *Icmf*^{fl/+}K^{LSL}LC (n = 24), *Icmf*^{fl/fl}K^{LSL}LC (n = 14), and control (n = 10) mice. Methylcellulose colony assay of bone marrow cells (B) and splenocytes (C) (n = 3 for each genotype) cultured in the absence of exogenous growth factors. (D) Photographs from typical experiment in panel C.

The K^{LSL}LC mice also express K-RAS^{G12D} in myeloid cells and exhibit signs of myeloproliferation, including an ability of hematopoietic cells to exhibit autonomous colony growth in vitro. Consequently, bone marrow cells and splenocytes from *Icmf*^{fl/+}K^{LSL}LC mice consistently formed colonies in methylcellulose in the absence of exogenous growth factors (Figure 6B-D). However, colony growth of bone marrow cells and splenocytes from *Icmf*^{fl/fl}K^{LSL}LC mice was reduced by 94% ($P = .025$) and 98% ($P = .013$), respectively (Figure 6B-D).

Discussion

In previous studies, we showed that the inactivation of *Icmf* inhibited K-RAS-induced transformation of fibroblasts in vitro.¹¹ The current experiments reveal that conditional inactivation of *Icmf* ameliorates phenotypes of K-RAS-induced malignancies in vivo and suggest that ICMT could be a potential target in the treatment of K-RAS-induced malignancies.

In our initial experiments, we used the *Mx1-Cre* transgene to produce mice with a K-RAS-induced MPD. The inactivation of *Icmf* in these mice reduced each of the major MPD phenotypes in vivo and virtually eliminated the autonomous growth of K-RAS^{G12D}-expressing myeloid and erythroid hematopoietic progenitors in vitro. However, despite the significant impact on MPD phenotypes, inactivating *Icmf* did not improve survival. One potential explanation for this finding is that the lethality of the MPD was not strictly related to the MPD phenotypes but to lesions in other tissues. The *Mx1-Cre*-induced activation of K-RAS^{G12D} is not restricted to the bone marrow and spleen and can produce severe lesions in multiple other tissues, albeit with incomplete penetrance. We suspected that the lower levels of *Cre* expression in those other tissues may have activated the latent K-RAS allele in some cells without inactivating both *Icmf* alleles. Indeed, genotyping of lesions in other tissues showed that *Icmf* was not fully inactivated. Another potential explanation for why inactivating *Icmf* did not improve survival is that the lethality of the MPD was related to inefficient erythropoiesis and anemia²³ and that inactivating *Icmf* failed to counteract this phenotype. Indeed, although inactivating *Icmf* normalized the EPO sensitivity of K-RAS^{G12D}-expressing hematopoietic cells in vitro, sick *Icmf*^{fl/+}K^{LSL}M and *Icmf*^{fl/fl}K^{LSL}M mice were anemic. In any case, the inactivation of *Icmf* clearly improved survival in the lysozyme M-*Cre* transgene model.

This study supports previous findings that the absence of *Icmf* causes oncogenic K-RAS-expressing fibroblasts to proliferate

slowly.^{11,24} Similarly, inactivation of *Icmf* almost eliminated the ability of K-RAS^{G12D}-expressing myeloid and erythroid progenitors to form CFU-GM and BFU-E colonies in methylcellulose without exogenous growth factors. However, in the presence of growth factors, *Icmf*-deficient bone marrow cells produced more colonies, regardless of K-RAS mutation status. The increased colony production of *Icmf*-deficient bone marrow cells was limited to the myeloid lineage (the majority of colonies were CFU-GMs). This finding raises a potential issue of unwanted side effects with ICMT inhibitor drugs. On the other hand, the increased colony production in *Icmf*-deficient cells was observed only at saturating concentrations of growth factors, making it somewhat improbable that hematopoietic cell proliferation and differentiation would be affected in vivo. In line with that view, mice lacking *Icmf* in hematopoietic cells (with wild-type K-RAS) exhibit normal white blood cell counts and differentials over many months of observation (A.M.W. and M.O.B., unpublished data, 2007).¹¹ We do not have an explanation for the increased colony production of *Icmf*-deficient bone marrow cells, but the results are reminiscent of a previous study, which showed that inactivation of the CAAX protein endoprotease RCE1 increased white blood cell counts.²⁵ However, this analogy is not perfect, as the absence of *Rce1* actually accelerates the development and progression of K-RAS-induced MPD, increases splenomegaly and tissue infiltration, and reduces survival.²⁰ Thus, the inactivation of RCE1 and ICMT, which act sequentially on the CAAX protein substrates, yields different results.

Why did *Rce1* deficiency accelerate and *Icmf* deficiency inhibit the K-RAS-induced MPD? One possibility could be that, in addition to the CAAX proteins, a subset of the RAB proteins (ie, the ones terminating with -CXC) are processed by ICMT but not by RCE1.^{24,26} The RAB proteins regulate the transport and targeting of vesicles and organelles within cells.²⁷ Thus, it is conceivable that that carboxyl methylation of the CXC-RAB proteins is important for K-RAS-induced oncogenesis in vivo and that inactivating *Icmf* interferes with this function.

Inactivating *Icmf* mislocalized the RAS proteins in K-RAS^{G12D}-expressing splenocytes, but a substantial amount was still associated with the membrane fraction. Previous studies using GFP-tagged RAS constructs showed that most of the RAS proteins are found on the plasma membrane in wild-type cells but are found in the cytosol and on internal membranes in *Icmf*-deficient fibroblasts.¹⁰ Thus, the RAS proteins found in the P100 fraction in *Icmf*-deficient cells are most probably associated with internal membranes, such as the Golgi. Finding RAS proteins associated

with membranes in *Icmt*-deficient cells is not surprising because they are farnesylated and retain the secondary membrane-targeting signals (ie, palmitoylation in the case of H- and N-RAS and a polylysine motif in the case of K-RAS). Regardless, the inactivation of *Icmt* had a significant impact on most of the phenotypes elicited by K-RAS^{G12D} in hematopoietic cells.

The effect of the *Icmt* inactivation on the proliferation of fibroblasts and hematopoietic cells was probably not caused by variations in RAS expression levels: the expression of K-RAS and total RAS was similar in *Icmt*^{Δ/+}K^{G12D} and *Icmt*^{Δ/Δ}K^{G12D} fibroblasts, and basal and stimulated RAS-GTP levels were similar in *Icmt*^{fl/+}K^{LSL}M and *Icmt*^{fl/fl}K^{LSL}M splenocytes.

Expression of K-RAS^{G12D} attenuated the GM-CSF-induced phosphorylation of MEK and ERK in CD11b-splenocytes. Attenuation of RAS-ERK signaling in response to endogenous oncogenic K-RAS has been observed in multiple cell types, such as fibroblasts and hematopoietic progenitors, and is now a relatively well-established finding.^{21,28,29} Interestingly, *Icmt* deficiency further reduced the GM-CSF-stimulated activation of MEK and ERK in CD11b-splenocytes. It is tempting to speculate that the reduced activation of MEK and ERK in splenocytes lacking *Icmt* was related to smaller spleens *in vivo* and reduced colony growth *in vitro*. However, this speculation would be limited to splenocytes because reduced activation of ERK was not observed in *Icmt*-deficient bone marrow cells in the current study or fibroblasts in previous studies.¹¹

In conclusion, inactivating *Icmt* interferes with the progression and severity of K-RAS-induced MPD *in vivo*. Several laboratories are working to develop potent ICMT inhibitors.¹²⁻¹⁴ Testing those compounds as antitumor agents will probably be aided by the models described here, which would make it

possible to compare, side by side, the impact of pharmacologic and genetic loss of ICMT activity.

Acknowledgments

The authors thank Tyler Jacks for providing the *Kras2^{LSL}* mice, Aziz Hussein for assistance with histopathology, and Birgitta Swolin for advice and discussions.

This study was supported by grants from the Swedish Medical Research Council, the Swedish Cancer Society, the Swedish Children's Cancer Fund, and Västra Götalandsregionen (M.O.B.); and by National Institutes of Health (grants CA099506 and AR050200) (S.G.Y.). M.O.B. is a fellow of the Royal Swedish Academy of Sciences and the European Hematology Association José Carreras Young Investigator Fellowship Program.

Authorship

Contribution: A.M.W. and B.A.C. designed and performed research and analyzed and interpreted data; M.L., A.L., A.-K.M.S., and K.M.E.A. performed research; C.K. analyzed data; S.G.Y. designed research and suggested revisions to the paper; and M.O.B. designed research and wrote the paper.

Conflict-of-interest disclosure: The authors declare no competing financial interests.

Correspondence: Martin O. Bergo, Wallenberg Laboratory, Institute of Medicine, Sahlgrenska University Hospital, S-413 45 Gothenburg, Sweden; e-mail: martin.bergo@wlab.gu.se.

References

- Rodenhuis S. ras and human tumors. *Semin Cancer Biol.* 1992;3:241-247.
- Bos JL. ras oncogenes in human cancer: a review. *Cancer Res.* 1989;49:4682-4689.
- Stirewalt DL, Radich JP. The role of FLT3 in hematopoietic malignancies. *Nat Rev Cancer.* 2003;3:650-665.
- Bollag G, Clapp DW, Shih S, et al. Loss of NF1 results in activation of the Ras signaling pathway and leads to aberrant growth in hematopoietic cells. *Nat Genet.* 1996;12:144-148.
- Pendergast AM, Quilliam LA, Cripe LD, et al. BCR-ABL-induced oncogenesis is mediated by direct interaction with the SH2 domain of the GRB-2 adaptor protein. *Cell.* 1993;75:175-185.
- Young SG, Ambroziak P, Kim E, Clarke S. Postisoprenylation protein processing: CXXX (CaaX) endoproteases and isoprenylcysteine carboxyl methyltransferase. In: Tamanoi F, Sigman DS, eds. *The Enzymes*. Vol. 21. San Diego: Academic Press; 2000;155-213.
- Kohl NE, Omer CA, Conner MW, et al. Inhibition of farnesyltransferase induces regression of mammary and salivary carcinomas in ras transgenic mice. *Nat Med.* 1995;1:792-797.
- Mahgoub N, Taylor BR, Gratiot M, et al. *In vitro* and *in vivo* effects of a farnesyltransferase inhibitor on Nf1-deficient hematopoietic cells. *Blood.* 1999;94:2469-2476.
- Whyte DB, Kirschmeier P, Hockenberry TN, et al. K- and N-Ras are geranylgeranylated in cells treated with farnesyl protein transferase inhibitors. *J Biol Chem.* 1997;272:14459-14464.
- Michaelson D, Ali W, Chiu VK, et al. Postisoprenylation CAAX processing is required for proper localization of Ras but not Rho GTPases. *Mol Biol Cell.* 2005;16:1606-1616.
- Bergo MO, Gavino BJ, Hong C, et al. Inactivation of *Icmt* inhibits transformation by oncogenic K-Ras and B-Raf. *J Clin Invest.* 2004;113:539-550.
- Donelson JL, Hodges HB, Macdougall DD, Henriksen BS, Hrycyna CA, Gibbs RA. Amide-substituted farnesylcysteine analogs as inhibitors of human isoprenylcysteine carboxyl methyltransferase. *Bioorg Med Chem Lett.* 2006;16:4420-4423.
- Anderson JL, Henriksen BS, Gibbs RA, Hrycyna CA. The isoprenoid substrate specificity of isoprenylcysteine carboxylmethyltransferase: development of novel inhibitors. *J Biol Chem.* 2005;280:29454-29461.
- Winter-Vann AM, Baron RA, Wong W, et al. A small-molecule inhibitor of isoprenylcysteine carboxyl methyltransferase with antitumor activity in cancer cells. *Proc Natl Acad Sci U S A.* 2005;102:4336-4341.
- Jackson EL, Willis N, Mercer K, et al. Analysis of lung tumor initiation and progression using conditional expression of oncogenic *K-ras*. *Genes Dev.* 2001;15:3243-3248.
- Clausen BE, Burkhardt C, Reith W, Renkawitz R, Förster I. Conditional gene targeting in macrophages and granulocytes using LysMcre mice. *Transgenic Res.* 1999;8:265-277.
- Sjogren AK, Andersson KM, Liu M, et al. GG-Tase-I deficiency reduces tumor formation and improves survival in mice with K-RAS-induced lung cancer. *J Clin Invest.* 2007;117:1294-1304.
- Braun BS, Tuveson DA, Kong N, et al. Somatic activation of oncogenic Kras in hematopoietic cells initiates a rapidly fatal myeloproliferative disorder. *Proc Natl Acad Sci U S A.* 2004;101:597-602.
- Chan IT, Kutok JL, Williams IR, et al. Conditional expression of oncogenic K-ras from its endogenous promoter induces a myeloproliferative disease. *J Clin Invest.* 2004;113:528-538.
- Wahlstrom AM, Cutts BA, Karlsson C, et al. Rce1 deficiency accelerates the development of K-RAS-induced myeloproliferative disease. *Blood.* 2007;109:763-768.
- Tuveson DA, Shaw AT, Willis NA, et al. Endogenous oncogenic K-ras (G12D) stimulates proliferation and widespread neoplastic and developmental defects. *Cancer Cell.* 2004;5:375-387.
- Kühn R, Schwenk F, Aguet M, Rajewsky K. Inducible gene targeting in mice. *Science.* 1995;269:1427-1429.
- Braun BS, Archard JA, Van Ziffle JA, Tuveson DA, Jacks TE, Shannon K. Somatic activation of a conditional KrasG12D allele causes ineffective erythropoiesis *in vivo*. *Blood.* 2006;108:2041-2044.
- Bergo MO, Leung GK, Ambroziak P, et al. Isoprenylcysteine carboxyl methyltransferase deficiency in mice. *J Biol Chem.* 2001;276:5841-5845.
- Aiyagari AL, Taylor BR, Aurora V, Young SG, Shannon KM. Hematologic effects of inactivating the Ras processing enzyme Rce1. *Blood.* 2003;101:2250-2252.
- Leung KF, Baron R, Ali BR, Magee AI, Seabra MC. Rab GTPases containing a CAAX motif are processed post-geranylgeranylation by proteolysis and methylation. *J Biol Chem.* 2007;282:1487-1497.
- Seabra MC, Wasmeier C. Controlling the location and activation of Rab GTPases. *Curr Opin Cell Biol.* 2004;16:451-457.
- Guerra C, Mijimolle N, Dhawahir A, et al. Tumor induction by an endogenous K-ras oncogene is highly dependent on cellular context. *Cancer Cell.* 2003;4:111-120.
- Van Meter ME, Diaz-Flores E, Archard JA, et al. K-RasG12D expression induces hyperproliferation and aberrant signaling in primary hematopoietic stem/progenitor cells. *Blood.* 2007;109:3945-3952.